

Sheng-Jiang Powder Alleviates Th17/Treg Immune Imbalance of Experimental Autoimmune Encephalomyelitis by Regulating the Fatty Acids Metabolism

Lulu Wu^{1,*}, Haoyou Xu², Hui Xia¹, Lilin Peng¹, Lulu Qin¹, Qian Gong^{3,4}, Min Zhao², Zhibing Wu⁵, Yuanqi Zhao², Zequan Zheng^{2,6,*}

¹The Second Clinical Medical College, Guangzhou University of Chinese Medicine, Guangzhou, Guangdong, People's Republic of China; ²The Second Affiliated Hospital of Guangzhou University of Chinese Medicine, Guangzhou, Guangdong, People's Republic of China; ³The First Clinical Medical College, Guangzhou University of Chinese Medicine, Guangzhou, Guangdong, People's Republic of China; ⁴Lingnan Medical Research Center, Guangzhou University of Chinese Medicine, Guangzhou, Guangdong, People's Republic of China; ⁵The First Affiliated Hospital of Guangzhou University of Chinese Medicine, Guangzhou, Guangdong, People's Republic of China; ⁶Doctoral Candidates with the Same Academic Level of Guangzhou University of Traditional Chinese Medicine, Guangzhou, Guangdong, People's Republic of China

*These authors contributed equally to this work

Correspondence: Zequan Zheng; Yuanqi Zhao, Email DoctorCheng@gzucm.edu.cn; zyq2022@gzucm.edu.cn

Background: Multiple sclerosis (MS) is one of the leading causes of disability among young people, and the immune imbalance between T helper cell 17 (Th17) and regulatory T cells (Tregs) plays a crucial role in its pathogenesis. Currently, MS treatment relies significantly on immunosuppressive drugs or glucocorticoids, which often have side effects and limitations in efficacy. Sheng-Jiang powder (SJP), a traditional Chinese medicine formula, has demonstrated anti-inflammatory effects and may offer a novel therapeutic option for MS.

Aim: This study aimed to investigate the therapeutic efficacy and underlying mechanism of SJP in myelin oligodendrocyte glycoprotein 35–55 (MOG35-55)-induced experimental autoimmune encephalomyelitis (EAE) mice.

Methods: The efficacy of SJP was assessed using the MOG35-55-induced EAE model. Disease severity was monitored based on the clinical symptoms, body weight, and pathological damage. Furthermore, Th17/Treg balance in the peripheral and central immune systems was assessed. Metabolomic analysis was performed to detect differential metabolites in serum, and the effects of fatty acids on the lipoxygenase (LOX) metabolic pathway were investigated.

Results: SJP alleviated MOG35-55-induced EAE symptoms and histological damage, restored the peripheral Th17/Treg immune balance, decreased pro-inflammatory cytokine levels, and increased anti-inflammatory cytokine levels. SJP intervention also influenced omega-3 polyunsaturated fatty acid (PUFA) metabolism and absorption in EAE mice, promoting an anti-inflammatory process associated with 12/15-lipoxygenase(12/15-LOX) upregulation and 5-lipoxygenase(5-LOX) downregulation.

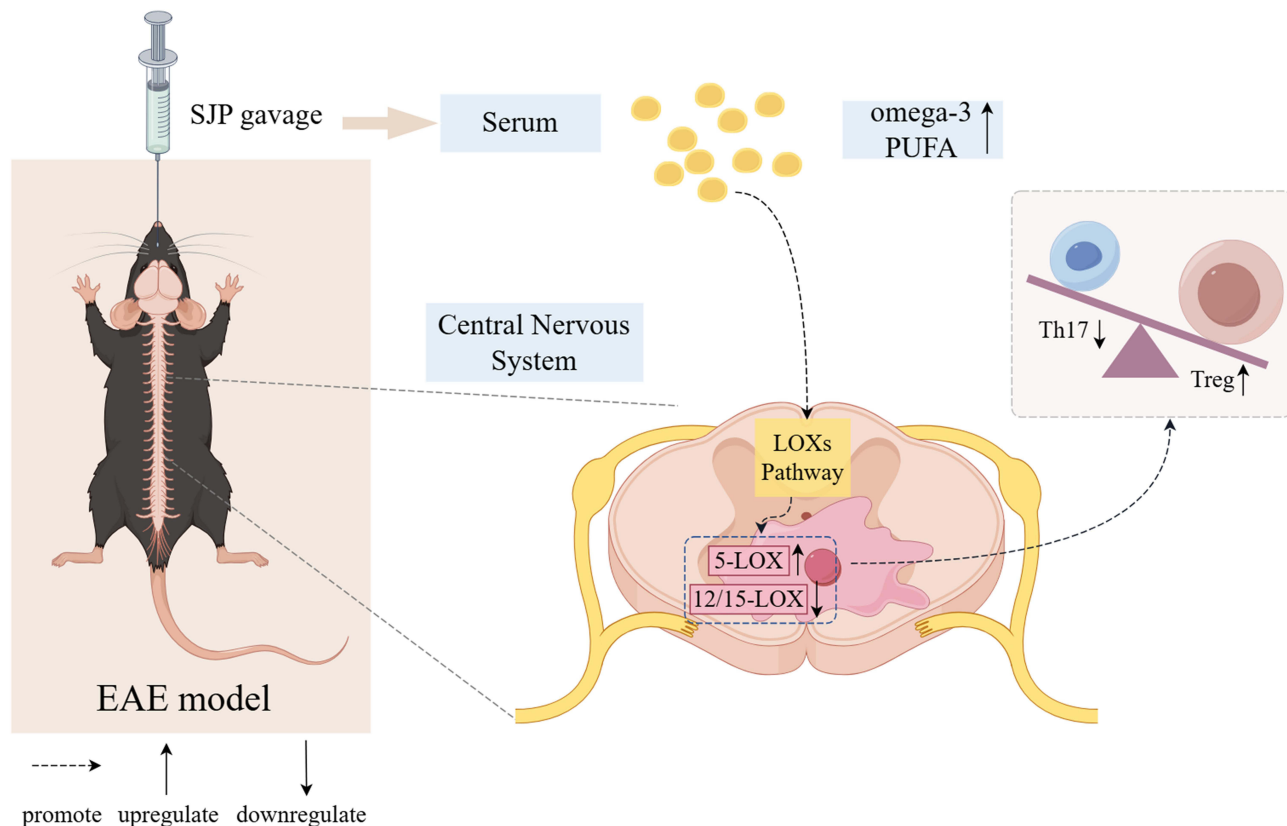
Conclusion: This study suggests that SJP is a viable treatment option for MS, and traditional Chinese medicine therapies for autoimmune diseases will continue to be developed.

Keywords: Shengjiang powder, multiple sclerosis, Th17/Treg, metabolomics, fatty acids metabolism

Introduction

Multiple sclerosis (MS) is an autoimmune disease that causes demyelination of the central nervous system (CNS), predominantly affecting the white matter of the brain, spinal cord, and optic nerve.¹ The latest survey revealed that the incidence rate of MS in China is 0.235/100000 per year and is gradually increasing.² This escalating incidence underscores the urgent need for novel pharmacological interventions. Short-term (3–4 weeks) intravenous or oral steroids are the recommended treatment options for acute-phase inflammatory responses in MS.^{3,4} Furthermore, numerous disease-modifying therapies are

Graphical Abstract



available for relapsing-remitting MS (RRMS) or progressive MS that develops after the onset of RRMS. These treatments include interferons, glatiramer, teriflunomide, S1P receptor modulators, fumarates, cladribine, and several monoclonal antibodies.¹

Th17 and Tregs, both subtypes of CD4⁺ T cells, play distinct roles in the immune system. Th17 primarily orchestrate inflammatory responses, whereas Tregs function as immune suppressors. When a large number of Th17 infiltrate tissues, the balance between Th17 and Tregs is disrupted, which is closely associated with the onset and progression of autoimmune diseases.^{5–7} The expression of Th17 is inhibited, and the differentiation of CD4⁺T cells into Tregs is induced to protect against MS models.^{8,9} This suggests that balancing the Th17/Treg ratio is a crucial therapeutic target in MS. Accordingly, new therapeutic strategies that modulate Th17/Treg balance in the CNS are required to improve MS treatment options.

Recent studies have highlighted the crucial role of lipid metabolism in Th17 differentiation, as it supports membrane synthesis and regulates the function of these cells. These findings indicate potential targets for immune modulation.¹⁰ Notably, lipid derivatives LPE 1–18:1 have been demonstrated to reduce the infiltration of Th17 into the CNS of mice with EAE by regulating retinoic acid receptor-related orphan receptor gamma t (ROR γ t).¹¹ Besides, reducing the levels of oleic acid, a monounsaturated fatty acid, increases the likelihood of naive CD4⁺ cell differentiation into Tregs.¹² These findings provide promising insights into regulating Th17 and Tregs differentiation by modulating lipid metabolism, which may have implications for developing novel therapeutic strategies for immune-related disorders.

Traditional Chinese medicine (TCM) has demonstrated significant potential in treating immune disorders.¹³ These empirical formulations contain multiple components that exert therapeutic effects through multi-targeted drug models. SJP is a traditional Chinese formula documented in the Treatise on Febrile Diseases and Pestilence during the Ming

dynasty. It was composed of *Rheum officinale* Baill. (Dahuang, Chinese), *Curcuma longa* L (Jianghuang, Chinese), *Bombyx mori Linnaeus* (Jiangcan, Chinese), and *Cryptotympana pustulata Fabricius* (Chantui, Chinese). Among these, *Rheum officinale* Baill. and its active ingredients exhibit significant anti-inflammatory effects. In a cerebral ischemia-reperfusion model, *Rheum officinale* Baill. extract can alleviate blood-brain barrier dysfunction and improve the inflammatory response of the nervous system.¹⁴ Curcumin, a compound with neuroprotective and neuropharmacological effects, has significant potential for treating MS.¹⁵ *Bombyx mori Linnaeus* can improve scopolamine-induced Alzheimer's disease, indicating its beneficial effects in neurodegenerative diseases.¹⁶ Moreover, *Cryptotympana pustulata Fabricius* can ameliorate neuronal apoptosis in epileptic mice by modulating the PI3K/Akt/Nrf2 signaling pathway.¹⁷ Emodin, the main component of *Rheum officinale* Baill. in SJP, can exert its effects by regulating adenosine 5'-monophosphate-activated protein kinase (AMPK), peroxisome proliferator-activated receptor (PPAR), and inflammation-related signaling pathways, demonstrating promising therapeutic efficacy in the treatment of obesity, hyperlipidemia, and non-alcoholic fatty liver disease.¹⁸ Curcumin, the main component of *Curcuma longa* L, can regulate the levels of free fatty acids by affecting fatty acid synthesis, β -oxidation activities, and the desaturation system, potentially improving insulin resistance, obesity, and other FFA-related diseases.¹⁹ Therefore, SJP demonstrates the potential for anti-inflammatory action and fatty acid regulation. Our previous studies have provided compelling evidence that SJP mitigates CNS damage through multiple mechanisms, including preserving blood-brain barrier integrity,²⁰ suppressing the IL-6/JAK2/STAT3 signaling cascade in the brain,²¹ and modulating the Nrf2/HO-1/HIF-1 α pathway in the spinal cord.²² These studies highlight the potential of SJP in MS; however, its effects on Th17/Treg balance and lipid metabolism remain poorly understood.

The EAE model is the most commonly used animal model for studying MS.²³ EAE is induced by injecting specific myelin-associated antigens such as myelin basic protein, myelin oligodendrocyte glycoprotein (MOG), and proteolipid protein. These antigens stimulate the immune system of animals to attack their neural tissue. The pathophysiology of the EAE model is primarily mediated by sensitized CD4⁺ T cells, manifested by mononuclear cell infiltration around small blood vessels in the CNS and demyelination.²⁴ This model is ideal for studying MS because of its high similarity in pathological features, disease processes, and immunological responses to clinical MS. In this study, we used the EAE model to investigate the effect of SJP on Th17/Treg balance, explore its mechanisms, and discover how fatty acid metabolism affects EAE and Th17/Treg regulation.

Materials and Methods

Medicine Preparation

The SJP medicinal granules, prepared and supplied by Guangdong Yifang Pharmaceutical Co., Ltd., comprised *Rheum officinale* Baill. (Dahuang, batch number: A2050681), *Curcuma longa* L (Jianghuang, batch number: A2011471), *Bombyx mori Linnaeus* (Jiangcan, batch number: A2092181), and *Cryptotympana pustulata Fabricius* (Chantui, batch number: A2082271). The herbs were converted into medicinal granules after boiling, filtering, concentrating, and drying. Medicinal granules were packed in a specification in which 1 g of granules was equivalent to 4 g (*Rheum officinale* Baill.), 5.5 g (*Curcuma longa* L), 3 g (*Bombyx mori Linnaeus*), and 6 g (*Cryptotympana pustulata Fabricius*) of herbs. The aforementioned medicinal granules were mixed according to the proportions listed in Table 1 and dissolved in water. The clinical dosage of SJP for adults is 0.03 g/kg, equivalent to 6.165 g/kg for mice, and it was considered a low dose.

Table 1 Component Herbs of SJP

Botanical Plant Name	Chinese Name	Part Used	Composition (% w/w)	Place of Origin	Test Report Number
<i>Rheum officinale</i> Baill.	Da Huang	Root and rhizome	40	Gansu, China	NO.220512C2024
<i>Curcuma longa</i> L.	Jiang Huang	Rhizome	30	Yunnan, China	NO.220121C2016
<i>Bombyx mori</i> Linnaeus	Jiang Can	Entire Body	20	Gansu, China	NO.220922C2046
<i>Cryptotympana pustulata</i> Fabricius	Chan Tui	Cast-off shell	10	Anhui, China	NO.220901C2024

Abbreviation: SJP, Sheng Jiang missing . Please indicate where it shPowders.

The high dose was 12.33 g/kg. Prednisone acetate tablets were prepared and supplied by Zhejiang Xianju Pharmaceutical Co., Ltd (batch number: H33021207) and dissolved in pure water to a concentration of 6 mg/kg for backup.

Ultra-High Performance Liquid Chromatography-MS/MS(UPLC-MS/MS) Analysis of SJP

The active ingredients detection of SJP was performed using UPLC-MS/MS. SJP samples were thawed from -80°C storage and homogenized by vortexing for 1 minute before detection. A 70% methanolic aqueous extractant containing internal standard, pre-chilled at -20°C , was vortex-mixed for 15 minutes. Centrifugation at 12,000 revolutions per minute under 4°C conditions for 3 minutes yielded a supernatant filtered through $0.22\ \mu\text{m}$ microporous membranes for LC-MS/MS analysis. The instrumental setup comprised a UPLC system (ExionLC™ AD, <https://sciex.com.cn/>) coupled with a tandem mass spectrometry (MS/MS). Chromatographic separation was achieved using an Agilent SB-C18 column ($1.8\ \mu\text{m}$, $2.1\ \text{mm} \times 100\ \text{mm}$), with mobile phase A being ultrapure water containing 0.1% formic acid and mobile phase B being acetonitrile containing 0.1% formic acid. The elution gradient was set to start with a B phase ratio of 5% at 0.00 min, linearly increasing to 95% within 9.00 min and maintaining for 1 minute, then decreasing to 5% from 10.00 to 11.10 min, and equilibrating until 14 min. The flow rate was 0.35 mL/min, the column temperature was set at 40°C , and the injection volume was 2 μL .

For mass spectrometry conditions, an electrospray ionization (ESI) source was operated with the ion source temperature fixed at 550°C . The ion spray voltage was applied at 5500 V in positive ion mode and adjusted to $-4500\ \text{V}$ in negative ion mode. Gas pressures were optimized as follows: ion source gas I (GSI) 50 psi, gas II (GSII) 60 psi, and curtain gas (CUR) 25 psi. Collision-induced ionization was specified at high intensity. The triple quadrupole (QQQ) operated in multiple reaction monitoring (MRM) mode with collision gas (nitrogen) intensity selected as medium. Declustering potential (DP) and collision energy (CE) for each MRM transition were determined through parameter optimization. Dynamic MRM monitoring was implemented based on metabolite elution times.

Animal

Female C57/BL6 mice (6–8 weeks old, 18–20 g) were obtained from Guangdong Medical Laboratory Animal Center (License No. SCXK(Guangdong)2022–0002). The mice were housed in a special pathogen-free (SPF) rodent facility at the First Affiliated Hospital of Guangzhou University of Chinese Medicine. Within this facility, mice had unrestricted access to standard rodent chow and water. The temperature was maintained at $23 \pm 3\ ^{\circ}\text{C}$ with 40%–60% humidity, and the lighting was controlled on a 12-h light/dark cycle. All animal experiments were conducted according to the guidelines of the Animal Ethics Committee of the First Affiliated Hospital of Guangzhou University of Chinese Medicine (Ethics No.: TCMF1-2022063).

EAE Model Establishment and Treatment

Fifty female mice were randomly divided into five groups: control group (CON, $n=10$), EAE model group (MOD, $n=10$), low-dose SJP group (SJP-L, $n=10$), high-dose SJP group (SJP-H, $n=10$), and positive control group treated with prednisone acetate tablets (PAT, $n=10$). The neurobehavioral score served as the primary outcome measure. Sample size was calculated using PASS software with $\alpha=0.05$, 80% power, and balanced allocation across five groups, yielding a minimum requirement of 5 mice per group. Taking into account a 20% mortality, the software recommended a design of 7 samples per group ([Supplementary 2](#)). However, we ultimately selected 10 mice per group to address individual variability.

The EAE model was developed in accordance with an established protocol.^{25,26} All mice were subcutaneously injected with an antigen-mixed emulsion (200 μg of MOG35-55 emulsified in a 1:1 ratio with Complete Freund's Adjuvant (CFA) containing 4 mg/mL inactivated *Mycobacterium tuberculosis*) on day 0, followed by intraperitoneal injections of 500 ng Pertussis Toxin (PTX) (List Biological Labs, cat#179A, USA) on days 0 and 2, to induce EAE. From days 2–21, mice in the SJP-L and SJP-H groups received oral administration of SJP at concentrations of 6.165 g/kg and 12.33 g/kg, respectively. The PAT group received prednisone acetate tablets at a concentration of 6 mg/kg,²⁷ whereas mice in the CON and MOD groups received an equivalent volume of saline as a placebo.

Following the establishment of the EAE model, mice gradually lose weight and develop symptoms between 9–14 days, manifesting as weakness or even paralysis of the tail and limbs.²⁸ The EAE clinical score was assessed for each

animal according to the following criteria: 0 = no signs of disease, 0.5 = partial loss of tail tonus, 1 = loss of tail tonus, 2 = moderate hind limb paraparesis, 2.5 = severe hind limb paraparesis, 3 = partial hind limb paralysis, 3.5 = hind limb paralysis, 4 = tetraplegia, and 5 = death.²⁹ Apart from the control group, all EAE mice performed weight loss and had a clinical score of 0.5 or greater. Consequently, all these mice met the criteria for the EAE model and were thus included in the experiment, totaling 50 mice.

Behavioral Assessment

From Day 0 onwards, the body weight and clinical score were evaluated according to the standard mentioned in previous study.²⁹

Serum and Tissue Collection

On day 22, before the mice were euthanized, blood was collected and sited at room temperature for 2 h before centrifugation at 3000 rpm at 4 °C for 15 min. Following centrifugation, the supernatant was aspirated, repackaged, and stored at -80 °C for subsequent metabolomic analysis, serum immunoglobulin G (IgG) measurement, and Enzyme-Linked Immunosorbent Assay (ELISA). After euthanasia with pentobarbital sodium, the spleen, brain, and lumbar spinal cord tissues were collected and immediately frozen at -80 °C for further investigation.

Hematoxylin-Eosin (H&E) Staining

The brain and lumbar spinal cord were immersed in 4% paraformaldehyde for 24 h and embedded in paraffin. Tissue sections were stained with H&E to assess the degree of inflammatory damage. Two independent blinded investigators assessed inflammation according to the following standard, as described previously.³⁰ The slides were scanned using a Panoramic Midi digital slide scanner (3DHISTECH Ltd., Hungary), and lesions were evaluated with CaseViewer 2.4 (3DHISTECH Ltd).

Immunohistochemistry (IHC)

Paraffin-embedded brains and lumbar spinal cord tissues were cut into 4- μ m sections, repaired with citrate, rinsed, washed in phosphate buffer saline (PBS), and permeabilized in hydrogen peroxide at room temperature for 10 min. The sections were incubated with anti-Inducible Nitric Oxide Synthase (iNOS) (Abcam, ab49999, 1:200) and Arginase-1 (Arg-1) (Abcam, ab239731, 1:200) at 4 °C overnight, followed by incubation with Horseradish Peroxidase (HRP)-conjugated goat anti-mouse IgG (zsbio, PV-9000, 1:5000) at 37 °C for 30 min. The slices were washed with PBS and stained with diaminobenzidine (DAB). The whole slides were scanned by a Panoramic Midi digital slide scanner (3DHISTECH Ltd., Hungary), and lesions were evaluated with CaseViewer 2.4 (3DHISTECH Ltd).

Real-Time Polymerase Chain Reaction (RT-PCR) Assay

First, total RNA was extracted from the cortex and lumbar spinal cord tissues using the RNA Easy Fast Tissue/Cell RNA Extraction Kit (Tiangen, DP451, China). Second, the concentration and purity of the extracted RNA were measured using a NanoDrop (Thermo Scientific, USA). Third, the RNA was reverse-transcribed into DNA using the First-Strand cDNA Synthesis Kit (Tiangen, KR118, China). Finally, cDNA was amplified using the Talent qPCR SYBR Green PreMix Kit (Tiangen, FP209, China), and DNA amplification was performed using the ABI7500 Real-Time PCR Detection System (Thermo Scientific, USA). Primer sequences used are listed in Table 2. The results were analyzed using the $2^{-\Delta\Delta C_t}$ method.

ELISA Assay and Total IgG Detection

Serum concentrations of IL-10 (Elabscience, M0046c, China), IL-17A (Elabscience, M0047c, China), and TGF- β 1 (Beyotime Biotechnology, PT878, China) were measured using an ELISA kit. Serum IgG was detected using URIT-8021A automatic biochemical analyzer.

Table 2 Primer Sequence

Target/Control Gene	Primer Sequences
GAPDH	F 5'- CATCACTGCCACCCAGAAGACTG - 3' R 5'- ATGCCAGTGAGCTTCCCGTTCAG - 3'
Foxp3	F 5'- AGAAGCAGCGGACACTCAAT - 3' R 5'- CACTTGTGCAGACTCAGGTTGT - 3'
IL-10	F 5'- GCTCTTACTGACTGGCATGAG - 3' R 5'- CGCAGCTCTAGGAGCATGTG - 3'
IL-17A	F 5'- TCTCTGATGCTGTTGCTGCT - 3' R 5'- ACGTGGAACGGTTGAGGTAG - 3'
ROR γ t	F 5'- CAGAGACACCACCGGACATC - 3' R 5'- CCCAGATGACTTGTCCCCAC - 3'
TGF- β 1	F 5'- AGGGCTACCATGCCAACTTC - 3' R 5'- CCACGTAGTAGACGATGGGC - 3'

Detection of Serum Metabolites

Sample preparation and extraction for metabolomics

The serum stored at -80°C was thawed on ice and vortexed for 10 seconds. Subsequently, 50 μL of the sample and 300 μL of the extraction solution (ACN: Methanol = 1:4, v/v) containing internal standards were added to a 2 mL microcentrifuge tube. The samples were vortexed for 3 min and centrifuged at 12,000 rpm for 10 min at 4°C . Then, 200 μL of the supernatant was collected and placed at -20°C for 30 min, followed by centrifugation at 12,000 rpm for 3 min at 4°C . A 180 μL aliquot of the supernatant was transferred for liquid chromatography-mass spectrometry(LC-MS) analysis.

T3 UPLC Conditions

The sample extracts were analyzed using an LC-ESI-MS/MS system (UPLC, ExionLC AD; MS, QTRAP[®] System). The analytical conditions were as follows: UPLC column: Waters ACQUITY UPLC HSS T3 C18 (1.8 μm , 2.1 \times 100 mm); column temperature: 40°C ; flow rate: 0.4 mL/min; injection volume: 2 μL ; solvent system: water (0.1% formic acid) and acetonitrile (0.1% formic acid). The gradient program was 95:5 v/v at 0 min, 10:90 v/v at 11.0 min, 10:90 V/V at 12.0 min, 95:5 v/v at 12.1 min, and 95:5 v/v at 14.0 min.

Esi-Qtrap-Ms/Ms

Linear ion trap (LIT) and QQQ scans were conducted on a QTRAP[®] LC-MS/MS system equipped with an ESI Turbo Ion-Spray interface, operating in both positive and negative ion modes and controlled by Analyst 1.6.3 software (Sciex). The ESI source parameters included a source temperature of 500°C ; ion spray voltages of 5500 V (positive) and -4500 V (negative); and GSI settings of 55 psi, GSII settings of 60 psi, and CUR settings of 25 psi with high collision gas (CAD). Instrument tuning and mass calibration were performed using 10 and 100 $\mu\text{mol/L}$ polypropylene glycol solutions in QQQ and LIT modes. Specific MRM transitions were monitored based on the metabolites eluted during each period.

Metabolomics Data Analysis

Principal Component Analysis(PCA)

Unsupervised PCA was performed using the statistical function prcomp in R (www.r-project.org). The data were unit variance scaled before the analysis, as recommended by Chen et al.³¹

Hierarchical Cluster Analysis and Pearson Correlation Coefficients

The hierarchical cluster analysis (HCA) results for samples and metabolites were presented as heatmaps with dendrograms. Pearson correlation coefficients (PCC)³² between samples were calculated using R and were presented as heatmaps only. Both HCA and PCC were performed using the R package ComplexHeatmap. For HCA, we used unit-variance scaling for standardization to represent the normalized metabolite signal intensities as a color spectrum.

Differential Metabolites Selected

In our two-group analysis, we extracted variable importance in projection(VIP) values from the OPLS-DA results, including score and permutation plots, using the R program. Before the Orthogonal partial least squares-discriminant analysis(OPLS-DA) analysis, the data were log-transformed (\log_2) and mean-centered. To avoid overfitting, 200 permutations were performed.

KEGG Annotation and Enrichment Analysis

To map the identified metabolites to KEGG pathways, we annotated them using the KEGG compound database (<http://www.kegg.jp/kegg/compound/>). The importance of the significantly regulated pathways was determined using hypergeometric test *p*-values after metabolite set enrichment analysis.

Western Blot (WB) Analysis

Approximately 100 μg of spinal cord lysates, rich in proteins, was resolved on an SDS-PAGE gel for detailed separation. These samples were then subjected to WB using primary antibodies specific to 5-LOX (Proteintech, Cat No.10021-1-Ig, 1:1000) and peroxisome proliferators-activated receptors gamma(PPAR- γ) (Proteintech, Cat No.16643-1-AP, 1:1000). The resulting bands were visualized using a high-sensitivity molecular imaging system (Bio-Rad, Hercules, USA) after an optimal incubation period with the appropriate secondary antibodies. Subsequently, the intensities of these bands were quantitatively analyzed and calculated using ImageJ software for precise and accurate measurements.

Immunofluorescence Staining

The spinal cord was embedded in paraffin and sectioned into 4- μm slices. Non-specific binding was blocked with 3% Bovine Serum Albumin(BSA) for 1 h. The cells were incubated overnight at 4 °C with primary antibodies for iba-1 (Abcam, ab283319, 1:100), 5-LOX, and PPAR- γ (1:100). Alexa Fluor-conjugated secondary antibodies (1:500) were used for 1 h, and nuclei were counterstained with DAPI for clear visualization. The whole slides were scanned by a Panoramic Midi digital slide scanner (3DHISTECH Ltd., Hungary), and lesions were evaluated with CaseViewer 2.4 (3DHISTECH Ltd.)

Statistical Analysis

All statistical analyses were performed using Statistical Package for the Social Sciences software (version 25.0; IBM, Armonk, NY, USA). One-way analysis of variance was used for parametric data, and non-parametric data were analyzed using the Kruskal–Wallis test, followed by Bonferroni's test. The above results were visualized by GraphPad Prism software (version 8.4.3). Data are expressed as mean \pm standard deviation (SD). Statistical significance was set at $p < 0.05$.

Results

Results of UPLC-MS/MS Analysis

To guarantee the quality of the drug, we analyzed the chemical compounds in SJP, and a total of 1668 compounds were detected by SJP ([Supplementary 1](#)), including Chrysophanol-8-O-(6'-acetyl)-glucoside, Rhein-8-O-glucoside, and DL-Tryptophan. These compounds are mainly classified as follows: phenolic acids and tannins, flavonoids, anthraquinones, and organic acids. The top 20 substances in terms of relative content are shown in [Figure 1A](#) (negative ion mode) and [Figure 1B](#) (positive ion mode). The 20 compounds along with their basic molecular formulas and chemical structures are listed in [Table 3](#). Among the identified compounds, 18 components achieved a qualitative level of Level 1, while 2 components reached Level 2, signifying a high degree of confidence in the identification of these compounds.

SJP Alleviates Neurological Deficiency and Inflammatory Infiltration in MOG35-55-Induced EAE Model

This study aimed to investigate the effect of SJP on EAE in mice. After establishing the EAE model and intervention ([Figure 2A](#)), we observed that the first onset of EAE occurred at approximately D9 and gradually worsened over the following days. Compared with the CON group, the clinical score on D11–D21 significantly increased in the MOD

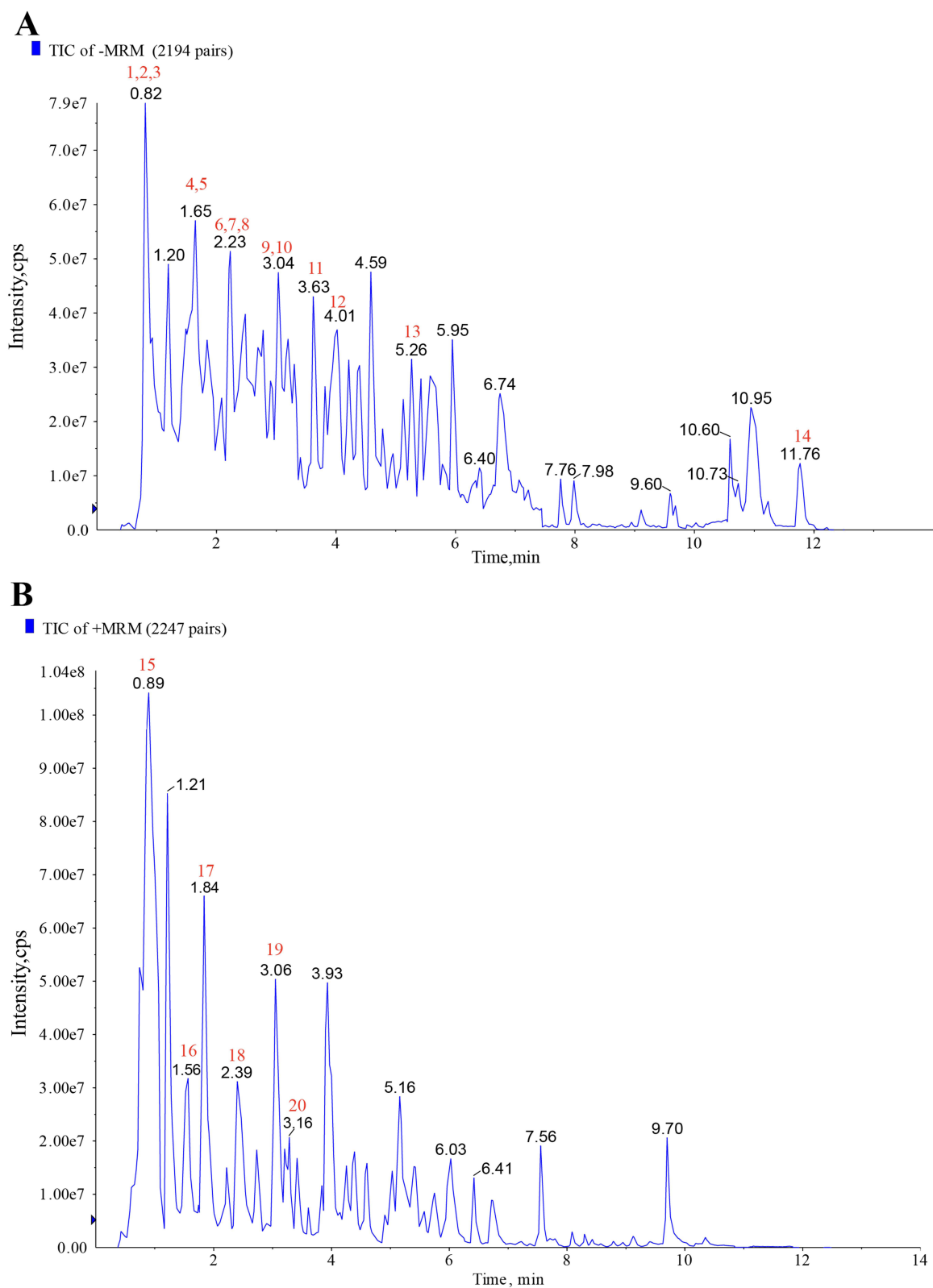
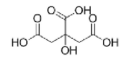
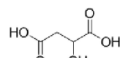
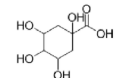
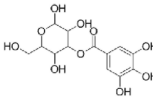
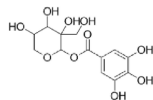
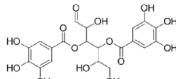
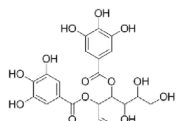
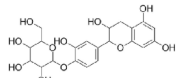
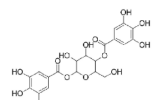


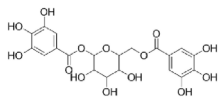
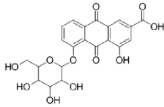
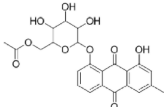
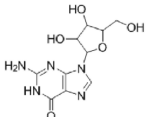
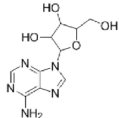
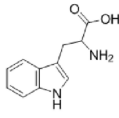
Figure 1 The top 20 components of SJP. **(A)** Total ion chromatogram of SJP in negative ion mode. **(B)** Total ion chromatogram of SJP in positive ion mode.

Table 3 The Top 20 Components of SJP

Peak name	Retention Time(min)	m/z(experiment)	Precursor type	Level	Compound Name	Chemical Structure
1	0.9	191.0198	[M-H]-	I	Citric Acid	
2	1	133.0142	[M-H]-	I	L-Malic acid	
3	1.1	191.0560	[M-H]-	2	Quinic Acid	
4	1.5	331.0675	[M-H]-	I	3-O-Galloyl-D-glucose	
5	1.6	331.0686	[M-H]-	I	5-O-Galloyl-D-hamamelose	
6	2.1	483.0779	[M-H]-	I	3,4-Di-O-Galloyl-D-Glucose	
7	2.3	483.0788	[M-H]-	I	2,3-Di-O-Galloyl-β-D-Glucose	
8	2.2	451.1258	[M-H]-	I	Epicatechin-4'-O-β-D-glucopyranoside	
9	2.8	483.0797	[M-H]-	I	1,4-Di-O-Galloyl-D-glucose	

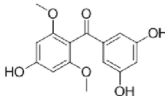
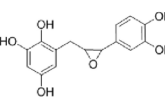
(Continued)

Table 3 (Continued).

Peak name	Retention Time(min)	m/z(experiment)	Precursor type	Level	Compound Name	Chemical Structure
10	3	483.0790	[M-H]-	2	1,6-Di-O-galloyl-β-D-glucose	
11	3.7	445.0772	[M-H]-	I	Rhein-8-O-glucoside	
12	4.1	163.0400	[M-H]-	I	2-Hydroxycinnamic acid	
13	5.3	457.1151	[M-H]-	I	Chrysophanol-8-O-(6'-acetyl)-glucoside	
14	11.7	255.2330	[M-H]-	I	Cetostearic acid	
15	0.9	116.0702	[M+H]+	I	4-Methylazetidine-2-Carboxylic acid	
16	1.5	284.0995	[M+H]+	I	Guanosine	
17	1.8	268.1044	[M+H]+	I	9-Alpha-Ribofuranosyladenine	
18	2.4	205.0971	[M+H]+	I	DL-Tryptophan	

(Continued)

Table 3 (Continued).

Peak name	Retention Time(min)	m/z(experiment)	Precursor type	Level	Compound Name	Chemical Structure
19	3	291.0869	[M+H] ⁺	I	(3,5-dihydroxyphenyl)-(4-hydroxy-2,6-dimethoxyphenyl)methanone	
20	3.2	291.0869	[M+H] ⁺	I	Katsumadin	

Notes: Level 1: Indicates that the sample material's MS/MS spectrum (all fragment ions of the material) and Retention time match the database material with a score of 0.7 or above. Level 2: Represents a match between the sample material's MS/MS spectrum (including all fragment ions) and Retention time with the database material, scoring between 0.5 and 0.7.

group. SJP and PAT groups exhibited significantly lower scores than the MOD group (Figure 2B). Furthermore, the MOD group (around D16) developed obvious symptoms of hind limb paralysis earlier than the SJP and PAT groups (around D18). Interestingly, the body weight of EAE mice gradually declined compared with that of the CON group and reached its lowest point at D9, the time of the first onset. However, during D18–D21, it dropped rapidly again with aggravation of the disease in the MOD group. Conversely, SJP and PAT groups continued to increase (Figure 2C).

H&E staining of the brain and lumbar spine demonstrated that inflammatory cells infiltrated the vascular and subcortex regions in both the brain and lumbar spine when compared to the CON group (Figure 2D). In some severe cases, aggregation of inflammatory cells occurs in the brain parenchyma and spinal cord. This phenomenon was significantly reduced by SJP and PAT treatments. (Figure 2E and F). In conclusion, the CNS exhibited an inflammatory collapse in the MOG35-55-induced EAE model, and lumbar enlargement was more severe. These findings suggest that SJP can alleviate EAE by ameliorating neurological deficiency and inflammatory infiltration.

SJP Reestablishes the Peripheral Th17/Treg Homeostasis

To investigate the mechanism of action of SJP, we used ELISA and total IgG detection to assess the Th17/Treg axis in EAE mice. A Th17/Treg imbalance is considered a hallmark of MS and is involved in the course of the disease.^{33,34} Elevated Th17 levels in the serum and CNS are specific markers of MS and EAE. These inflammatory cells are known for their toxic effects on the blood-brain barrier and neurons while continually stimulating glial cells to recruit peripheral immune cells to invade the CNS.^{35,36}

In our study, we initially observed that the spleens of the EAE mice were significantly enlarged. The SJP treatment mitigated this enlargement (Figure 3A and B). Consistent with this observation, serum levels of IL-17A, TGF- β 1, and IgG were significantly higher in the MOD group than in the CON group. Conversely, IL-10 levels were significantly lower in the MOD group. Importantly, SJP treatment significantly reduced the secretion of IL-17A, TGF- β 1, and IgG in the serum while increasing IL-10 levels (Figure 3C–F). These findings suggest that SJP may exert therapeutic effects in EAE by modulating the Th17/Treg axis, thereby reducing inflammation and alleviating disease symptoms.

SJP Alleviates Inflammation of the CNS

In addition to investigating the effects of SJP on peripheral immunity, we examined its effects on CNS immunity. We measured the cytokine levels and counted iNOS (+) and Arg-1 (+) cells in the cerebral cortex and lumbar enlargement of mice using RT-PCR and IHC. When immune cells and pro-inflammatory mediators from peripheral circulation activate glial cells in the CNS, they elicit local inflammatory responses. Glial cells secrete neurotoxic substances, such as iNOS,

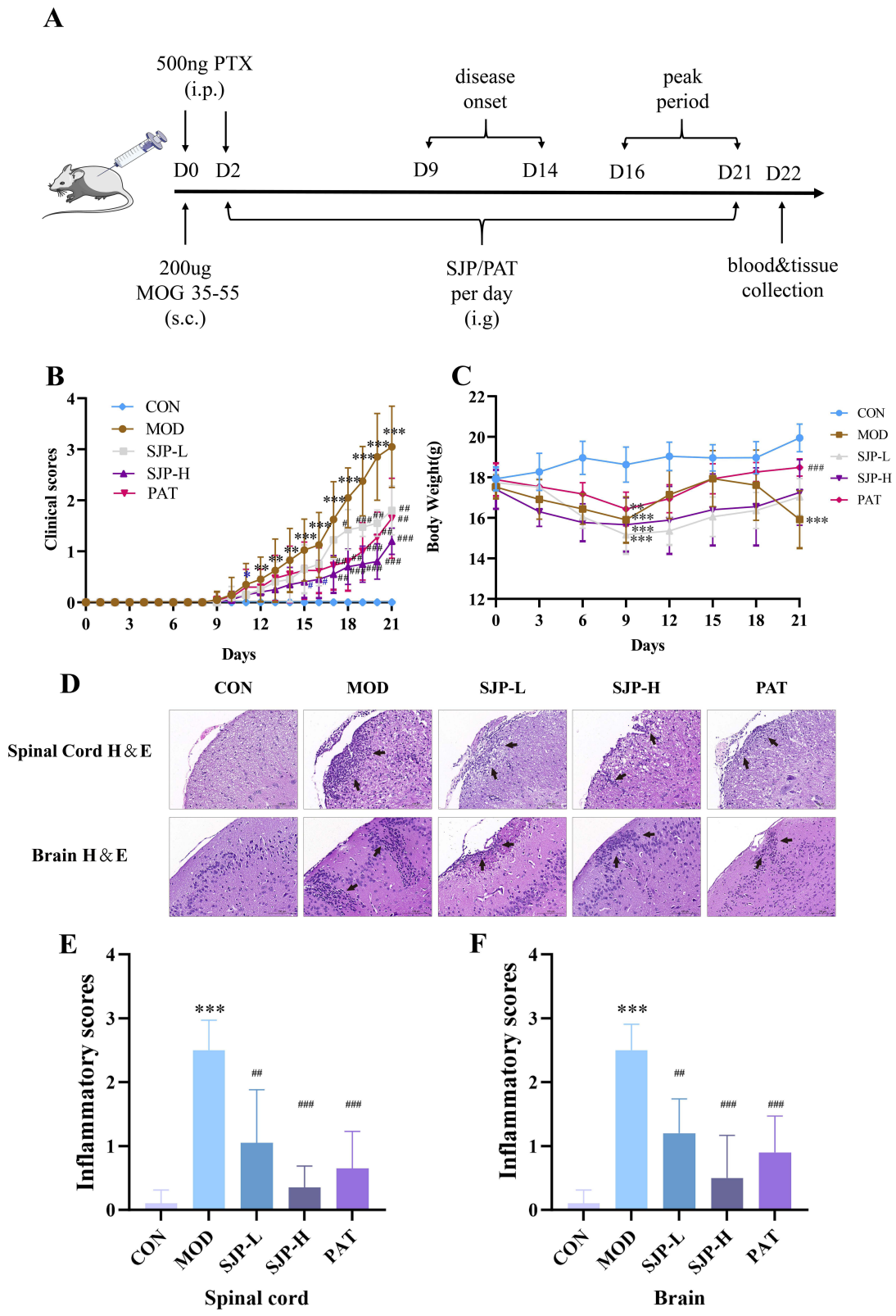


Figure 2 Effects of SJP on neurological deficiency and central nervous system histopathology in the EAE model. **(A)** Experimental protocol for MOG35-55-induced EAE model and treatment. **(B)** SJP and PAT groups demonstrated significantly delayed and less increase in clinical scores (n = 10). **(C)** Changes in mouse body weight over time among the five intervention groups (n = 10). **(D)** Histopathology of the lumbar spinal cord and brain slices stained with H&E (scale bar: 100 μm) were compared among CON, MOD, SJP-L, SJP-H, and PAT groups on day 22 post-immunization and the inflammatory scores (n = 10). **(E and F)** were calculated to statistics. Values are expressed as mean ± SD (n = 10). *p < 0.05, **p < 0.01, ***p < 0.001, compared with CON group; #p < 0.05, ###p < 0.01, ####p < 0.001, compared with MOD group.

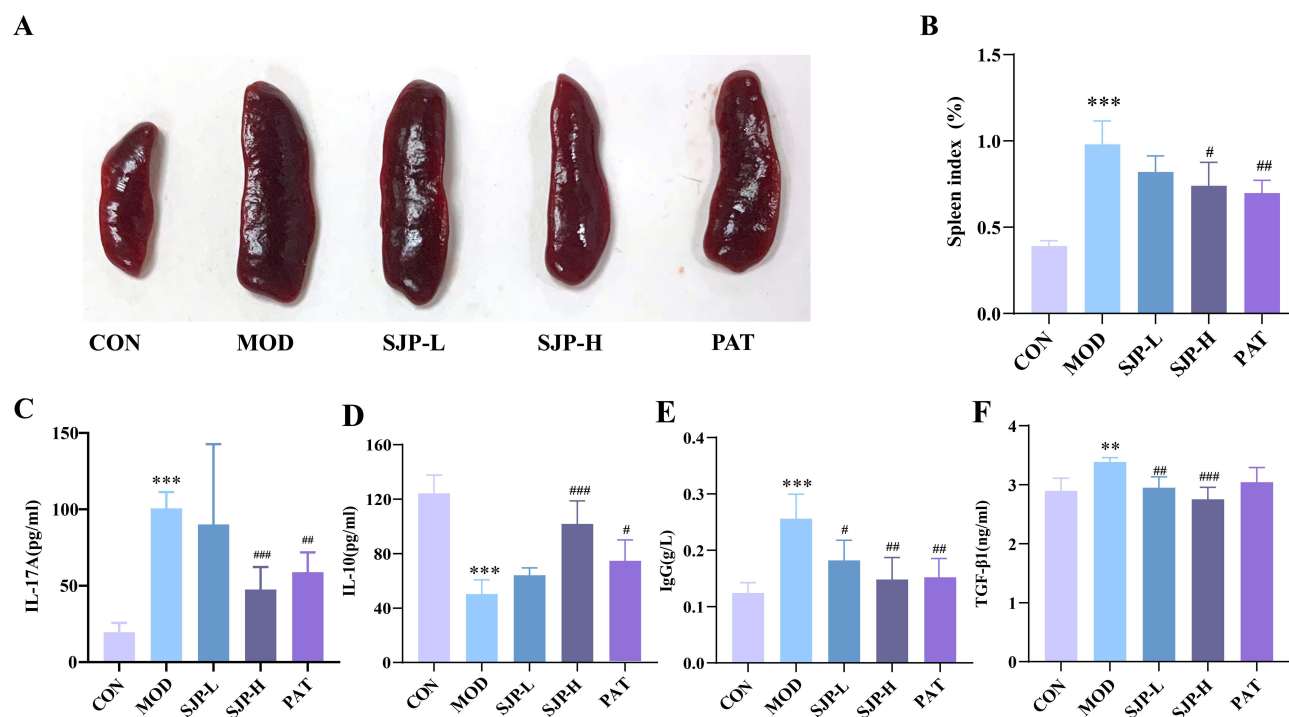


Figure 3 Effects of SJP on peripheral immunity. **(A and B)** Spleen indices (n = 6). **(C)** Serum level of IL-17A (n = 6). **(D)** serum level of IL-10 (n = 7). **(E)** serum level of TGF-β1 (n = 6). **(F)** serum level of IgG (n = 5). Values are expressed as mean ± SD. * $p < 0.05$, ** $p < 0.01$, *** $p < 0.001$, compared with the CON group; # $p < 0.05$, ### $p < 0.01$, #### $p < 0.001$, compared with the MOD group. Each repeat was performed independently.

which induce oxidative stress and inflammatory damage to tissues. Simultaneously, they secrete anti-inflammatory substances, such as Arg-1, which participate in tissue repair processes.³⁷

Compared to the CON group, the mRNA levels of IL-17A, ROR γ t, and TGF-β1 were overexpressed in both the cortex and spinal (Figure 4A–J). Conversely, mRNA levels of IL-10 and Foxp3 were low. Treatment with SJP and PAT significantly reduced the mRNA expression of these pro-inflammatory cytokines (IL-17A, ROR γ t, and TGF-β1), whereas the expression of anti-inflammatory factors (IL-10 and Foxp3) increased. In the MOD group, the number of iNOS (+) and Arg-1 (+) cells was higher than that in the CON group, whereas SJP and PAT reduced the activation of microglia and macrophages (Figure 4K). In summary, we speculate that SJP may reduce inflammatory damage in the CNS by alleviating Th17/Treg dysfunction and reducing microglial activation.

SJP Affects Fatty Acid Metabolism

To investigate the potential metabolic pathways and endogenous metabolic alterations of EAE by SJP, we performed a serum metabolomic analysis of CON, MOD, and SJP-H groups. Metabolic aberrations can affect the pathogenesis of MS and EAE by affecting T cell differentiation and the inflammatory microenvironment and may provide clues for exploring new therapeutic strategies.³⁸

A total of 928 metabolites were detected, and a PCA plot (Figure 5A) demonstrated a clear separation between CON and MOD groups and between SJP-H and MOD groups. Notably, the SJP-H group partially overlapped both groups, indicating that SJP altered organismal metabolism in EAE. The detected metabolites primarily consisted of amino acids and their metabolites, organic acids, fatty acyl groups, glycerophospholipids, and benzene (Figure 5B).

To accurately detect differences in metabolites, OPLS-DA was performed to estimate the metabolic differences in the serum of mice among the three groups. Compared with the MOD group, 54 metabolites in SJP-H were significantly adjusted, with 30 being fatty acyl groups (Figure 5C and D). This indicates that fatty acyl groups may be key metabolites for SJP in easing the immune disorder and inflammatory environment associated with EAE. The top ten compounds with

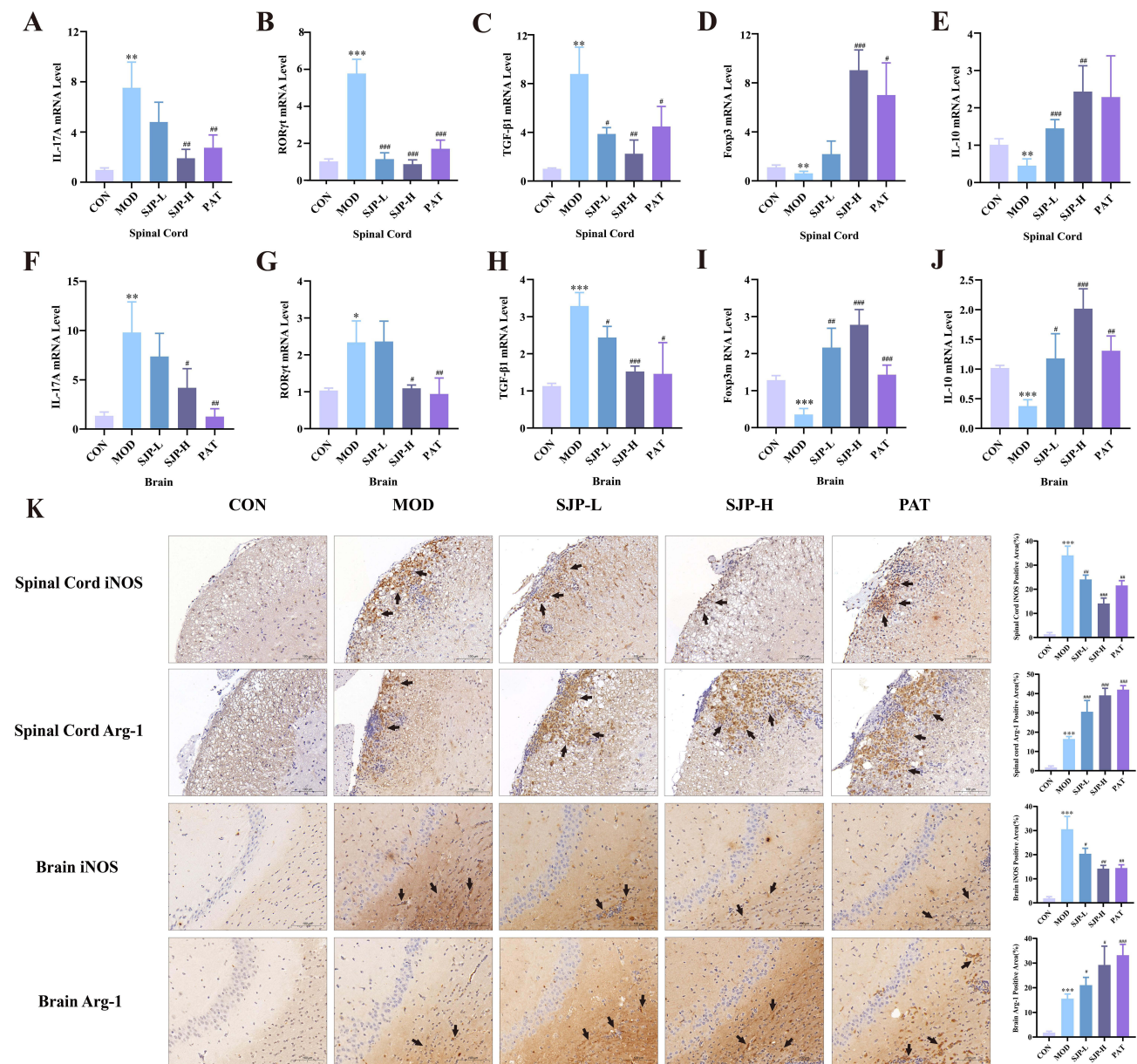


Figure 4 SJP treatment suppresses inflammation in the spinal cord and cerebral cortex of EAE mice. **(A–J)** Relative levels of IL-17A, ROR γ t, TGF- β 1, Foxp3, and IL-10 in the lumbar spinal and cerebral cortex were compared among groups on day 22 post-immunization by qRT-PCR ($n = 6$). **(K)** Lumbar spinal and brain tissues were stained with anti-iNOS and anti-Arg-1 antibodies by ICH, and their expression levels were measured by calculating the positive area ($n = 6$, scale bar: 100 μ m). Values are expressed as mean \pm SD. * $p < 0.05$, ** $p < 0.01$, *** $p < 0.001$, compared with the CON group; # $p < 0.05$, ## $p < 0.01$, ### $p < 0.001$, compared with the MOD group. Each repeat was performed independently.

significant differences were mainly Omega-3 unsaturated fatty acids derived from HOTrE, HDoHE, HDHA, HEPE, and others, and there was an upward trend (Table 4).

Metabolic pathway enrichment analysis suggested that SJP partially regulated the metabolic environment of EAE through arachidonic acid (AA) metabolism, C5-branched dibasic acid metabolism, butanoate metabolism, bile secretion, and carbon metabolism pathways. Among these pathways, AA metabolism was the most closely related to fatty acid metabolism (Figure 5E). Changes in the concentrations of specific metabolites, including 13(S)-HOTrE(γ), EPA, (\pm)12-HEPE, (\pm)12-HETE, (\pm)15-HETE, and (\pm)17-HDHA, are presented in Figure 5F.

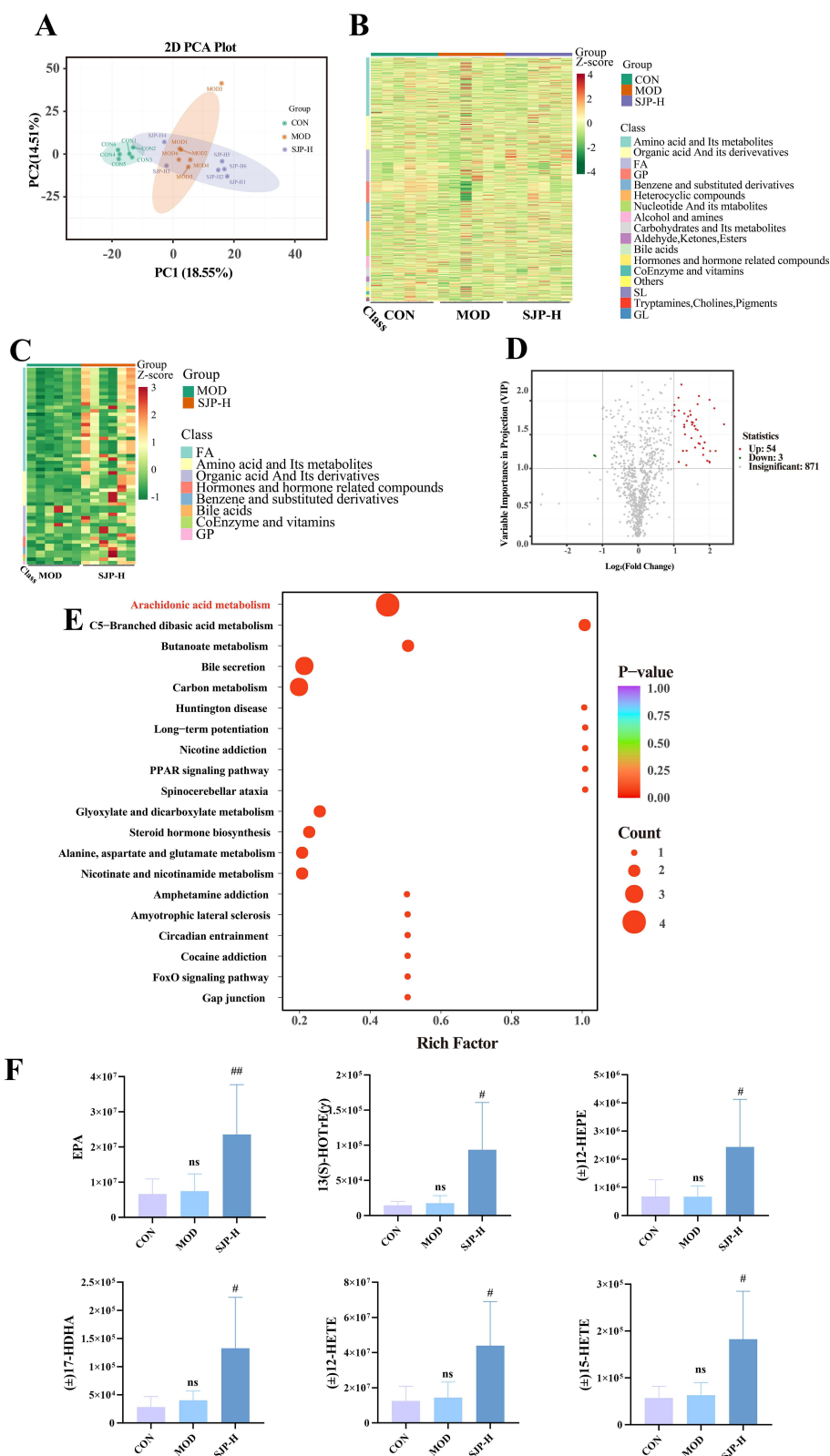


Figure 5 Data assessment of CON, MOD, and SJP-H samples from metabolomics. **(A)** PCA results: the y-axis indicates the secondary principal component, and the x-axis indicates the principal component ($n = 6$). **(B)** Cluster analysis of CON, MOD, and SJP-H groups ($n = 6$). **(C)** Cluster analysis of MOD and SJP-H groups. The expression levels of metabolites are distinguished by different colors; red indicates higher metabolite concentration, and green indicates lower metabolite concentration ($n = 6$). **(D)** Volcano plots of the metabolites in MOD and SJP-H groups. The red points represent upregulated metabolites, and the blue points represent downregulated metabolites. **(E)** KEGG pathway enrichment analysis of MOD and SJP-H groups. The larger the dot, the more enriched, and the redder the color, the smaller the p -value. **(F)** Concentration of the metabolites in the serum. Values are expressed as mean \pm SD. * $p < 0.05$, ** $p < 0.01$, *** $p < 0.001$, compared with the CON group; # $p < 0.05$, ## $p < 0.01$, ### $p < 0.001$, compared with the MOD group. Each repeat was performed independently.

Table 4 Summary of Top 10 Different Metabolites Screened According to Log2FC

No.	Formula	Compounds	Classification	Log2FC		Trend	
				MOD vs SJP-H	CON vs MOD	MOD vs SJP-H	CON vs MOD
1	C18H30O3	13(S)-HOTrE(γ)	FA	2.41	2.72	up	insig
2	C22H30O2	FFA(22:7)	FA	2.17	5.62	up	insig
3	C11H20N2O3	Pro-Ile	Amino acid and Its metabolites	2.14	-5.72	up	insig
4	C22H32O3	11-HDoHE	FA	2.02	5.82	up	insig
5	C22H32O3	8-HDoHE	FA	2	5.37	up	insig
6	C18H30O3	13-HOTrE	FA	2	5.97	up	insig
7	C22H32O3	16-HDoHE	FA	1.99	6.27	up	insig
8	C22H32O3	14(S)-HDHA	FA	1.94	6.81	up	insig
9	C20H30O3	(\pm)12-HEPE	FA	1.86	-3.11	up	insig
10	C20H30O3	(\pm)15-HEPE	FA	1.86	-3.11	up	insig

Abbreviation: FA, Fatty acid.

SJP Modulates the Th17/Treg Axis Through the Lipoxygenases (LOXs) Pathway

KEGG analysis revealed that the AA metabolic network emerged as the primary pathway through which the drug exerts its therapeutic effects. Lipoxygenases (LOXs) and their subsequent enzymes play pivotal roles in catalyzing PUFAs. Particularly, 5-lipoxygenase (5-LOX) serves as a crucial generator of pro-inflammatory leukotrienes (LTs), whereas 12/15-lipoxygenase (12/15-LOX) is indispensable for modulating Th17/Treg balance.^{39,40} To elucidate the mechanism by which SJP modulates inflammatory responses via the LOXs pathway, we assessed the expression levels of 5-LOX and 12/15-LOX in peripheral blood. Our findings revealed that the model group exhibited elevated serum levels of 5-LOX compared with the normal group, which was significantly reduced by SJP treatment (Figure 6A). Although the decrease in 12/15-LOX in the model group was not statistically significant, SJP significantly increased its concentration (Figure 6B and C). In the spinal cord tissue, we observed a decrease in the fatty acid transcription factor PPAR- γ in MOD, which was reversed in SJP. This suggests that SJP facilitates the uptake and utilization of PUFAs (Figure 6D). Furthermore, the expression patterns of 5-LOX and 12/15-LOX in the spinal cord tissue were consistent with those observed in the peripheral blood (Figure 6D). Based on these metabolomic findings, we hypothesized that SJP regulates fatty acid uptake, synthesis, and metabolism by upregulating omega-3 fatty acid levels. This action counteracts inflammatory responses by promoting the expression of 12/15-LOX and inhibiting 5-LOX.

Abnormal microglial activation is a key factor in CNS inflammatory responses in EAE model.⁴¹ Studies have indicated that 5-LOX facilitates the accumulation of inflammatory mediators by inducing microglial inflammation and recruiting neutrophils, contributing to EAE.⁴² Our findings revealed elevated 5-LOX expression in lesion tissues accompanied by decreased PPAR- γ levels, suggesting that 5-LOX and PPAR- γ are key targets of SJP.

To further elucidate the relationship between these targets and microglial activation, we conducted fluorescent double staining to assess the expression of 5-LOX, PPAR- γ , and iba-1+ cells in the spinal cord. The results demonstrated that the MOD group had an increased co-expression of 5-LOX compared to the CON group, which was reduced following SJP intervention (Figure 6E). Conversely, PPAR- γ exhibited the opposite trend, with increased expression in the SJP group compared to that in the MOD group (Figure 6F). We hypothesized that SJP, by upregulating beneficial fatty acids, activates PPAR- γ in microglia and downregulates 5-LOX, thereby modulating inflammatory responses in the central nervous tissue.

Discussion

This study investigated the efficacy and mechanism of SJP in alleviating EAE using a combination of behavioral observation experiments and serum metabolomics. Behavioral experiments were performed to record the neurological function scores of the mice to evaluate the improvement effect of SJP. Metabolomic analysis revealed the role of SJP in regulating fatty acid metabolism, comprehensively detected metabolic changes, and screened for potential biomarkers

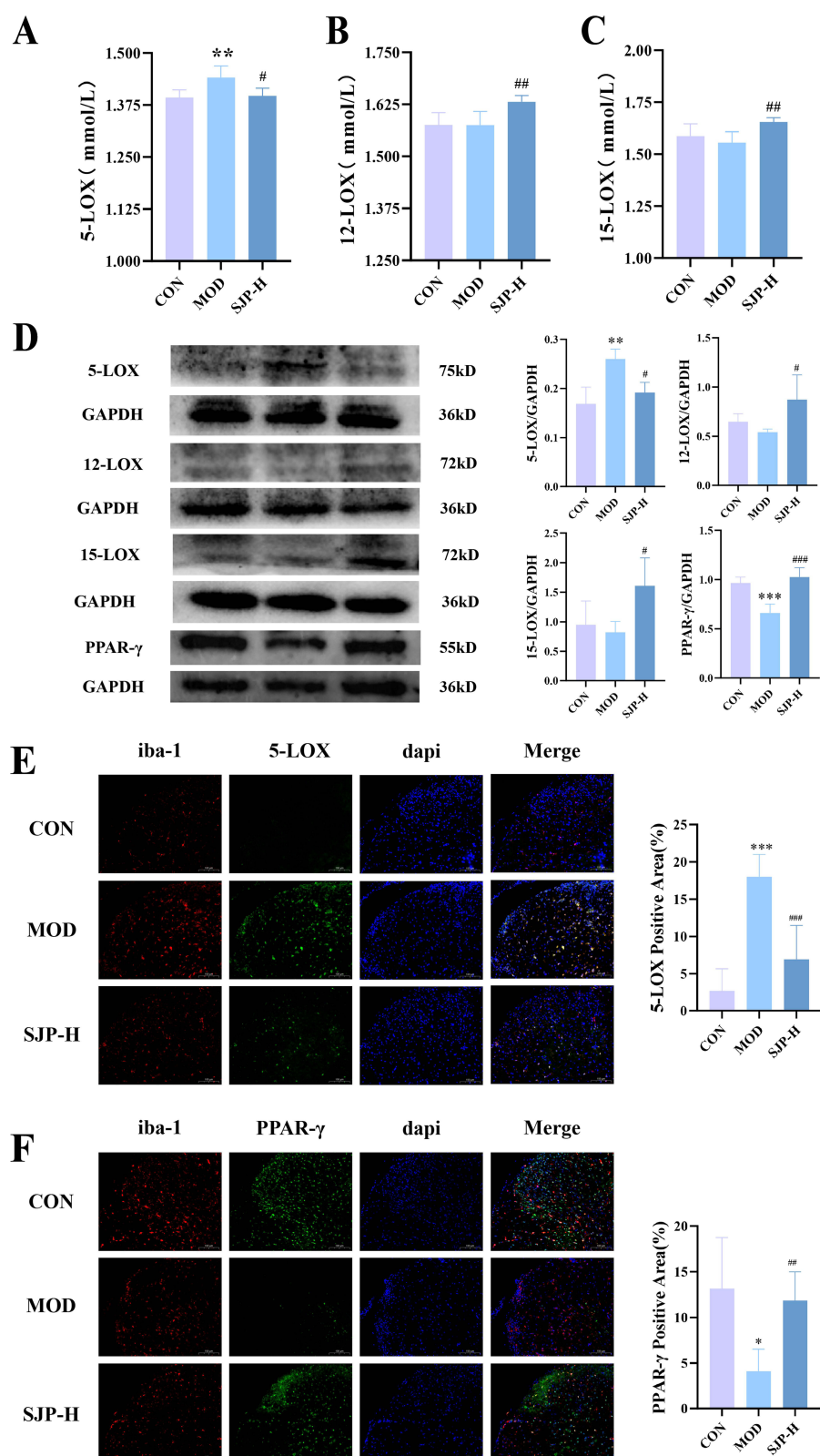


Figure 6 Effect of SJP on the LOXs pathway. Expression of (A) 5-LOX (n = 6), (B) 12-LOX (n = 6), and (C) 15-LOX (n = 6) in the serum. (D) The protein relative expression of 5-LOX, 12-LOX, 15-LOX, and PPAR- γ in the spinal cord (n = 5). The (E) 5-LOX, (F) PPAR- γ , and Iba-1 co-expression in the spinal cord. (n = 6). Values are expressed as mean \pm SD.* p < 0.05, ** p < 0.01, *** p < 0.001, compared with the CON group; # p < 0.05, ## p < 0.01, ### p < 0.001, compared with the MOD group. Each repeat was performed independently.

related to the progression or efficacy of EAE. Combining metabolomic and behavioral results revealed a potential relationship between metabolic changes and neuroinflammation, providing important clues for mechanistic studies. Previous studies have demonstrated that SJP possesses anti-inflammatory properties and has the potential to regulate fatty acid metabolism. Based on this, we hypothesized that SJP could modulate inflammation by regulating fatty acid metabolism. As shown in the graphical abstract, our findings indicate that SJP significantly reduced the levels of inflammatory factors in the spinal cord and brain tissues of EAE model mice and decreased inflammatory cell infiltration. Serum metabolomic analysis revealed that SJP significantly altered the composition of fatty acid metabolites, regulated the AA metabolic pathway, increased the levels of omega-3 PUFAs, and adjusted the expression of key enzymes in the LOXs signaling pathway. These findings support our hypothesis that SJP influences immune and inflammatory responses by modulating fatty acid metabolism.

Although TCM has been widely used to treat immune diseases,¹³ TCM studies of MS and EAE are limited. The present study is noteworthy because it identifies SJP as an effective therapeutic modality for EAE through rodent models and its integration with serum metabolomics to elucidate the underlying functional mechanisms, thus providing insights into drug development for MS. The significant findings of our study were as follows: the herbal compound SJP ameliorated neurological impairment in EAE mice and reduced inflammatory cell infiltration in both the cerebral cortex and lumbar spinal cord. SJP suppresses the production of pro-inflammatory cytokines by Th17 by rebalancing the peripheral Th17/Treg ratio and stimulating Tregs to secrete anti-inflammatory factors. This process reduces peripheral cellular invasion of the CNS and limits microglial activation.

Furthermore, metabolomic analysis revealed that SJP significantly alters fatty acid metabolism in EAE models, particularly by increasing omega-3 unsaturated fatty acids. The modulation of fatty acid metabolism may be a pivotal mechanism underlying the pharmacological action of SJP. Subsequent experiments have demonstrated that SJP regulates the LOXs pathway by upregulating omega-3 fatty acids, thereby reducing the inflammatory response in microglia.

MS is a CD4⁺T lymphocyte-dominated immune disease of the CNS characterized by a Th17/Treg immune imbalance.⁴³ Under the combined induction of transforming growth factor β 1 (TGF- β 1) and interleukin-6/interleukin-21 (IL-6/IL-21), the activated signal transducer and activator of transcription 3 (STAT3) directs naive T cells to express ROR γ t, which subsequently initiates T cell differentiation into Th17 subsets.³⁶ Activated Th17 disrupt the blood-brain barrier (BBB) by secreting inflammatory cytokines, such as IL-17A and IL-6, resulting in myelin loss and neuronal damage.⁴⁴ The pro-inflammatory factor IL-17A is typically present at higher concentrations in the serum, cerebrospinal fluid, and demyelinating lesions of patients with MS or EAE animals.³⁴ Conversely, Tregs exert immunomodulatory effects by secreting anti-inflammatory cytokines such as IL-10 and IL-35, alleviating MS or EAE symptoms.⁴⁵

Tregs differentiation and phenotype maintenance depend on STAT5 activation and Foxp3 expression. STAT5 and STAT3 regulate the dynamic Th17/Treg balance by competing with each other.⁴⁶ The resultant Tregs deficiency after activation initiates the loss of inhibitory function and Th17 proliferation, thereby weakening its inflammatory action due to the reduced secretion of the corresponding chemokines with migration capacity.⁴⁷ Additionally, this change was demonstrated by MOG antigen-induced changes in the central or peripheral immune system in EAE mice models. Consistent with previous studies, our results indicate that the Th17/Treg axis was disrupted in EAE mice. This phenomenon is manifested by defects in Th17 proliferation and Tregs function in the serum, accompanied by CNS changes and varying peripheral cytokine levels. Moreover, the cerebral cortex and lumbar bulge exhibited significant inflammatory cell infiltration and microglial activation in the EAE mice, indicating that SJP can improve MS symptoms. Collectively, our results demonstrated the therapeutic potential of SJP in MS. However, the underlying metabolic and molecular mechanisms remain elusive.

The onset, progression, and ultimate outcomes of MS are closely associated with environmental and dietary factors. Numerous studies have identified the presence of complex metabolic disorders in patients with MS/EAE.⁴⁸ Non-targeted metabolomics can effectively profile metabolic changes in organisms and is now used to identify pharmacological responses and relevant biomarkers in Chinese medicine.⁴⁹ Our study focused on the serum metabolites of EAE mice treated with SJP-treated EAE mice to elucidate their metabolic mechanisms. Previous results revealed that high-dose SJP was more effective in alleviating EAE symptoms and improving abnormal indices. Therefore, we selected SJP-H, CON, and MOD groups for extensive non-targeted metabolomic analysis. After SJP treatment, 54 metabolites were upregulated, and three were downregulated in EAE mice serum. Over half (55.56%) of these upregulated metabolites were fatty

acids, whereas the top 10 were mainly omega-3 PUFAs. Fatty acid metabolism plays a pivotal role in autoimmune disease development. It is often called the body's "metabolic cytokine", playing multifaceted roles in the etiology and pathogenesis of MS and EAE.⁵⁰ Besides, KEGG enrichment analysis revealed that fatty acid metabolism might regulate disease progression through multiple metabolic pathways, such as AA metabolism, inflammatory mediator regulation of transient receptor potential (TRP) channels, PPAR signaling pathway, and linoleic acid metabolism.

Omega-3 PUFA-based diets, particularly those rich in fish oil, can reduce the risk of MS and modulate MS-related inflammatory factors.⁵¹ In animal models, omega-3 fatty acids demonstrate potent immunomodulatory properties. Specifically, docosahexaenoic acid (DHA) and eicosapentaenoic acid (EPA), two primary omega-3 fatty acids, can inhibit the activation and secretion of pro-inflammatory cytokines by peripheral blood mononuclear cells (PBMC), Th1, and Th17. These fatty acids can differentiate naive T cells into Foxp3⁺-induced Treg cells (iTreg).^{52,53} Furthermore, a diet rich in DHA and EPA improved neurological deficits and increased PPAR- α , γ , and β/δ subtype expression, which are key receptors for lipid metabolism in CNS CD4⁺T cells, while reducing CNS CD4⁺T cell infiltration and pro-inflammatory factor secretion in EAE mice.^{53,54} Our findings indicated a Th17/Treg axis imbalance in the peripheral nervous system and CNS after EAE onset and abnormal pro-and anti-inflammatory cytokine secretion. The partial reversal of these outcomes by SJP may be because it improves PUFA metabolism and absorption in EAE mice, particularly omega-3, which inhibits Th17 activation and induces Tregs proliferation.

Exogenous PUFAs are metabolized by LOXs, resulting in various oxidized lipid and fatty acid derivatives that regulate the immune and inflammatory responses. For instance, 5-LOX converts AA into pro-inflammatory LTs, activating microglia and promoting cytokine secretion, such as IL-1 β and TNF- α .⁵⁵ In the EAE model, 5-LOX inhibition significantly improved clinical symptoms by suppressing Th1/Th17 differentiation and facilitating the transition of microglia to a protective M2 phenotype.⁵⁶ Conversely, 12/15-LOX exerted anti-inflammatory effects on EAE. Research has indicated that 12/15-LOX regulates dendritic cell maturation, and its deficiency can worsen Th17-mediated EAE progression.³⁹ Additionally, 12/15-LOX promotes Tregs.⁴⁰

However, the composition of SJP is complex and diverse. Studies have demonstrated that various active components in SJP possess anti-inflammatory and neurorestorative functions. Quinones, such as Rhein, significantly inhibit the release of proinflammatory factors by targeting the PI3K/Akt, ERK1/2, and TLR4/NF- κ B pathways⁵⁷ and activating the PPAR γ /histone deacetylase 3(HDAC3) complex to block NF- κ B acetylation.⁵⁸ Its congener, Chrysophanol, reduces the production of inflammatory mediators like IL-1 β through the PI3K/Akt/mTOR pathway, improving Intracerebral hemorrhage.⁵⁹ Phenolic acids, including Gallic acid derivatives, regulate Th17 immune responses and upregulate anti-inflammatory factors such as IL-10 and TGF- β , demonstrating immune balance modulation in atopic dermatitis models.⁶⁰ Additionally, Epicatechin alleviates neurodegenerative diseases by inhibiting abnormal tau protein phosphorylation and regulating β -amyloid protein metabolism.⁶¹ The multicomponent formulation of SJP exerts a synergistic anti-inflammatory effect through multiple pathways, and its effects on suppressing neuroinflammation and promoting repair align closely with the findings of this study.

Our study indicates that SJP treatment enhances omega-3 PUFA levels and modulates Th17/Treg immune balance through the 12/15-LOX and 5-LOX pathways, inhibiting microglial inflammation. This suggests a promising, low-side-effect alternative therapy for patients with MS and provides valuable insights into herbal treatments for MS. This study has some limitations. Although this study focused on the effects of SJP on lipid metabolism in EAE mice, further research is required to clarify how SJP affects lipid metabolism. The main active ingredients of SJP are not yet clear, and further studies should be conducted to explore the components of these four herbs accurately. In conclusion, SJP can be therapeutic in EAE mice by regulating Th17/Treg balance and lipid metabolism.

Conclusions

In conclusion, our study demonstrated the efficacy of SJP in EAE mice by maintaining the balance between the peripheral nervous system and the CNS Th17/Treg axis. Our serum metabolomic findings suggest that SJP primarily alters fatty acid metabolism in EAE mice and exerts therapeutic effects by affecting multiple metabolic pathways, including AA metabolism. SJP also enhances the levels of PUFAs, particularly omega-3 PUFAs, which helps regulate the balance between 12/15-LOX and 5-LOX. This modulation contributes to the improvement of the Th17/Treg immune imbalance.

Abbreviations

Arg-1, arginase 1; CFA, complete Freund's adjuvant; CNS, central nervous system; IL-6, interleukin 6; CON, control; EAE, experimental autoimmune encephalomyelitis; HCA, hierarchical cluster analysis; H&E, Hematoxylin-Eosin Staining; HIF-1 α , hypoxia inducible factor-1 α ; HO-1, heme oxygenase 1; HPLC, high-performance liquid chromatography; IHC, immunohistochemistry; IL-6, interleukin 6; IL-10, interleukin 10; IL-17A, interleukin 17A; iNOS, inducible nitric oxide synthase; JAK2, just another kinase 2; KEGG, Kyoto encyclopedia of genes and genomes; 5-LOX, 5-lipoxygenase; 12/15-LOX, 12/15-lipoxygenase; MOD, EAE model; MOG35-55, myelin oligodendrocyte glycoprotein 35-55; MS, Multiple sclerosis; Nrf2, nuclear factor erythroid 2-related factor 2; PAT, Prednisone acetate tablets; PCA, principal component analysis; PPAR- γ , peroxisome proliferator-activated receptor gamma; PTX, pertussis toxin; ROR γ t, receptor-related orphan receptor gamma t; RT-PCR, Real-time polymerase chain reaction; SJP, Sheng-jiang powder; SJP-L, SJP low-dose; SJP-H, SJP high-dose; TGF- β 1, transforming growth factor- β 1; Th17, T helper cell 17; Tregs, regulatory T cells.

Author Contributions

All authors made a significant contribution to the work reported, whether that is in the conception, study design, execution, acquisition of data, analysis and interpretation, or in all these areas; participated in drafting, revising or critically reviewing the article; gave final approval of the version to be published; have agreed on the journal to which the article has been submitted; and agreed to be accountable for all aspects of the work.

Funding

Natural Science Foundation of Guangdong Province (NO: 2022A1515220134), National Natural Science Foundation of China (NO: 82374390), Guangzhou Science and Technology Plan Project (NO: 2024A03J0037), Traditional Chinese Medicine Discipline Basic Theory Research of Guangzhou University of Chinese Medicine “Unveiling the List and Leading the Way” Project (NO: A1-2606-23-415-111Z20).

Disclosure

Lulu Wu and Zequan Zheng are co-first authors for this study. All authors declare no competing interests in this work.

References

- Marcus R. What is multiple sclerosis? *JAMA*. 2022;328(20):2078. doi:10.1001/jama.2022.14236
- Tian DC, Zhang C, Yuan M, et al. Incidence of multiple sclerosis in China: a nationwide hospital-based study. *Lancet Reg Health West Pac*. 2020;1:100010. doi:10.1016/j.lanwpc.2020.100010
- McGinley MP, Goldschmidt CH, Rae-Grant AD. Diagnosis and treatment of multiple sclerosis: a review. *JAMA*. 2021;325(8):765–779. doi:10.1001/jama.2020.26858
- Yamout B, Alroughani R, Al-Jumah M, et al. Consensus guidelines for the diagnosis and treatment of multiple sclerosis. *Curr Med Res Opin*. 2013;29(6):611–621. doi:10.1185/03007995.2013.787979
- Fujiwara M, Raheja R, Garo LP, et al. microRNA-92a promotes CNS autoimmunity by modulating the regulatory and inflammatory T cell balance. *J Clin Invest*. 2022;132(10). doi:10.1172/JCI155693
- Littman DR, Rudensky AY. Th17 and regulatory T cells in mediating and restraining inflammation. *Cell*. 2010;140(6):845–858. doi:10.1016/j.cell.2010.02.021
- Ulges A, Witsch EJ, Pramanik G, et al. Protein kinase CK2 governs the molecular decision between encephalitogenic TH17 cell and Treg cell development. *Proc Natl Acad Sci U S A*. 2016;113(36):10145–10150. doi:10.1073/pnas.1523869113
- Qu S, Hu S, Xu H, et al. TREM-2 drives development of multiple sclerosis by promoting pathogenic Th17 polarization. *Neurosci Bull*. 2024;40(1):17–34. doi:10.1007/s12264-023-01094-x
- Shi C, Zhang J, Wang H, et al. Trojan horse nanocapsule enabled in situ modulation of the phenotypic conversion of Th17 cells to treg cells for the treatment of multiple sclerosis in mice. *Adv Mater*. 2023;35(11):e2210262. doi:10.1002/adma.202210262
- Kanno T, Nakajima T, Miyako K, Endo Y. Lipid metabolism in Th17 cell function. *Pharmacol Ther*. 2023;245:108411. doi:10.1016/j.pharmthera.2023.108411
- Endo Y, Kanno T, Nakajima T, et al. 1-Oleoyl-lysophosphatidylethanolamine stimulates ROR γ t activity in T(H)17 cells. *Sci Immunol*. 2023;8(86):eadd4346. doi:10.1126/sciimmunol.add4346
- Lin L, Hu M, Li Q, et al. Oleic acid availability impacts thymocyte preprogramming and subsequent peripheral T(reg) cell differentiation. *Nat Immunol*. 2024;25(1):54–65. doi:10.1038/s41590-023-01672-1
- Ma HD, Deng YR, Tian Z, Lian ZX. Traditional Chinese medicine and immune regulation. *Clin Rev Allergy Immunol*. 2013;44(3):229–241. doi:10.1007/s12016-012-8332-0
- Mao M, Cao X, Liang Y, et al. Neuroprotection of rhubarb extract against cerebral ischaemia-reperfusion injury via the gut-brain axis pathway. *Phytomedicine*. 2024;126:155254. doi:10.1016/j.phymed.2023.155254

15. Rahiman N, Markina YV, Kesharwani P, Johnston TP, Sahebkar A. Curcumin-based nanotechnology approaches and therapeutics in restoration of autoimmune diseases. *J Control Release*. 2022;348:264–286. doi:10.1016/j.jconrel.2022.05.046
16. Guo YR, Jin H, Kim M, et al. Synergistic neuroprotective effects of mature silkworm and angelica gigas against scopolamine-induced mild cognitive impairment in mice and H(2)O(2)-induced cell death in HT22 mouse hippocampal neuronal cells. *J Med Food*. 2021;24(5):505–516. doi:10.1089/jmf.2020.4839
17. Zhang Q, Li RL, Tao T, et al. Antiepileptic effects of cicadae periostracum on mice and its antiapoptotic effects in H₂O₂-stimulated PC12 cells via regulation of PI3K/Akt/Nrf2 signaling pathways. *Oxid Med Cell Longev*. 2021;2021(1):5598818. doi:10.1155/2021/5598818
18. Yu L, Zhao Y, Zhao Y. Advances in the pharmacological effects and molecular mechanisms of emodin in the treatment of metabolic diseases. *Front Pharmacol*. 2023;14:1240820. doi:10.3389/fphar.2023.1240820
19. Nosrati-Oskouie M, Aghili-Moghaddam NS, Sathyapalan T, Sahebkar A. Impact of curcumin on fatty acid metabolism. *Phytother Res*. 2021;35(9):4748–4762. doi:10.1002/ptr.7105
20. Zheng Z, Lin X. The effect of Sheng-Jiang powder on immune inflammatory factors in EAE rats. *Traditional Chinese Drug Research and Clinical Pharmacology*. 2017;28(03):287–291.
21. Lyu BJ, Zheng ZQ, Zheng KN, et al. Therapeutic effect of Shengjiang Powder on experimental autoimmune encephalomyelitis mice through IL-6/JAK2/STAT3 signaling pathway: based on HPLC. *Zhongguo Zhong Yao Za Zhi*. 2022;47(12):3361–3371. doi:10.19540/j.cnki.cjcm.20211230.703
22. Wu L, Zheng Z, Zhao M, et al. The study on the regulatory effect of Sheng-Jiang powder on macrophages in EAE mice based on Nrf2/HO-1/HIF-1 α pathway. *Lishizhen Medicine and Materia Medica Research*. 2024;35(05):1118–1122.
23. Procaccini C, De Rosa V, Pucino V, Formisano L, Matarese G. Animal models of multiple sclerosis. *Eur J Pharmacol*. 2015;759:182–191. doi:10.1016/j.ejphar.2015.03.042
24. Constantinescu CS, Farooqi N, O'Brien K, Gran B. Experimental autoimmune encephalomyelitis (EAE) as a model for multiple sclerosis (MS). *Br J Pharmacol*. 2011;164(4):1079–1106. doi:10.1111/j.1476-5381.2011.01302.x
25. Shaw PJ, Barr MJ, Lukens JR, et al. Signaling via the RIP2 adaptor protein in central nervous system-infiltrating dendritic cells promotes inflammation and autoimmunity. *Immunity*. 2011;34(1):75–84. doi:10.1016/j.immuni.2010.12.015
26. Stromnes IM, Goverman JM. Active induction of experimental allergic encephalomyelitis. *Nat Protoc*. 2006;1(4):1810–1819. doi:10.1038/nprot.2006.285
27. Burton JM, O'Connor PW, Hohol M, Beyene J. Oral versus intravenous steroids for treatment of relapses in multiple sclerosis. *Cochrane Database Syst Rev*. 2012;12:CD006921. doi:10.1002/14651858.CD006921.pub3
28. Bittner S, Afzali AM, Wiendl H, Meuth SG. Myelin oligodendrocyte glycoprotein (MOG35-55) induced experimental autoimmune encephalomyelitis (EAE) in C57BL/6 mice. *J Vis Exp*. 2014;(86). doi:10.3791/51275-v
29. Quintana A, Muller M, Frausto RF, et al. Site-specific production of IL-6 in the central nervous system retargets and enhances the inflammatory response in experimental autoimmune encephalomyelitis. *J Immunol*. 2009;183(3):2079–2088. doi:10.4049/jimmunol.0900242
30. Wang X, Li B, Liu L, et al. Nicotinamide adenine dinucleotide treatment alleviates the symptoms of experimental autoimmune encephalomyelitis by activating autophagy and inhibiting the NLRP3 inflammasome. *Int Immunopharmacol*. 2021;90:107092. doi:10.1016/j.intimp.2020.107092
31. Chen Y, Zhang R, Song Y, et al. RRLC-MS/MS-based metabolomics combined with in-depth analysis of metabolic correlation network: finding potential biomarkers for breast cancer. *Analyst*. 2009;134(10):2003–2011. doi:10.1039/b907243h
32. Zhan H, Xiong Y, Wang Z, et al. Integrative analysis of transcriptomic and metabolomic profiles reveal the complex molecular regulatory network of meat quality in Enshi black pigs. *Meat Sci*. 2022;183:108642. doi:10.1016/j.meatsci.2021.108642
33. Fasching P, Stradner M, Graninger W, DeJaco C, Fessler J. Therapeutic potential of targeting the Th17/Treg axis in autoimmune disorders. *Molecules*. 2017;22(1):134. doi:10.3390/molecules22010134
34. Li YF, Zhang SX, Ma XW, et al. Levels of peripheral Th17 cells and serum Th17-related cytokines in patients with multiple sclerosis: a meta-analysis. *Mult Scler Relat Disord*. 2017;18:20–25. doi:10.1016/j.msard.2017.09.003
35. Kebir H, Kreyenborg K, Ifergan I, et al. Human TH17 lymphocytes promote blood-brain barrier disruption and central nervous system inflammation. *Nat Med*. 2007;13(10):1173–1175. doi:10.1038/nm1651
36. McGinley AM, Edwards SC, Raverdeau M, Mills K. Th17 cells, gammadelta T cells and their interplay in EAE and multiple sclerosis. *J Autoimmun*. 2018;87:97–108. doi:10.1016/j.jaut.2018.01.001
37. Voet S, Prinz M, van Loo G. Microglia in central nervous system inflammation and multiple sclerosis pathology. *Trends Mol Med*. 2019;25(2):112–123. doi:10.1016/j.molmed.2018.11.005
38. Zahoor I, Suhail H, Datta I, et al. Blood-based untargeted metabolomics in relapsing-remitting multiple sclerosis revealed the testable therapeutic target. *Proc Natl Acad Sci U S A*. 2022;119(25):e2123265119. doi:10.1073/pnas.2123265119
39. Rothe T, Gruber F, Uderhardt S, et al. 12/15-Lipoxygenase-mediated enzymatic lipid oxidation regulates DC maturation and function. *J Clin Invest*. 2015;125(5):1944–1954. doi:10.1172/JCI178490
40. Zamora A, Nogue M, Verdu L, et al. 15-Lipoxygenase promotes resolution of inflammation in lymphedema by controlling T(reg) cell function through IFN-beta. *Nat Commun*. 2024;15(1):221. doi:10.1038/s41467-023-43554-y
41. Distefano-Gagne F, Bitarafan S, Lacroix S, Gosselin D. Roles and regulation of microglia activity in multiple sclerosis: insights from animal models. *Nat Rev Neurosci*. 2023;24(7):397–415. doi:10.1038/s41583-023-00709-6
42. Chen S, Zou H. Lipoxygenase metabolism: critical pathways in microglia-mediated neuroinflammation and neurodevelopmental disorders. *Neurochem Res*. 2022;47(11):3213–3220. doi:10.1007/s11064-022-03645-6
43. Lee GR. The balance of Th17 versus Treg cells in autoimmunity. *Int J Mol Sci*. 2018;19(3):730. doi:10.3390/ijms19030730
44. Lu P, Cao Y, Wang M, et al. Mature dendritic cells cause Th17/Treg imbalance by secreting TGF-beta1 and IL-6 in the pathogenesis of experimental autoimmune encephalomyelitis. *Cent Eur J Immunol*. 2016;41(2):143–152. doi:10.5114/ceji.2016.60987
45. Wei X, Zhang J, Gu Q, et al. Reciprocal expression of IL-35 and IL-10 defines two distinct effector Treg subsets that are required for maintenance of immune tolerance. *Cell Rep*. 2017;21(7):1853–1869. doi:10.1016/j.celrep.2017.10.090
46. Lu HC, Kim S, Steelman AJ, et al. STAT3 signaling in myeloid cells promotes pathogenic myelin-specific T cell differentiation and autoimmune demyelination. *Proc Natl Acad Sci U S A*. 2020;117(10):5430–5441. doi:10.1073/pnas.1913997117
47. Danikowski KM, Jayaraman S, Prabhakar BS. Regulatory T cells in multiple sclerosis and myasthenia gravis. *J Neuroinflammation*. 2017;14(1):117. doi:10.1186/s12974-017-0892-8

48. Esposito S, Bonavita S, Sparaco M, Gallo A, Tedeschi G. The role of diet in multiple sclerosis: a review. *Nutr Neurosci.* 2018;21(6):377–390. doi:10.1080/1028415X.2017.1303016
49. Zhang A, Sun H, Wang Z, et al. Metabolomics: towards understanding traditional Chinese medicine. *Planta Med.* 2010;76(17):2026–2035. doi:10.1055/s-0030-1250542
50. Yu H, Bai S, Hao Y, Guan Y. Fatty acids role in multiple sclerosis as “metabokines”. *J Neuroinflammation.* 2022;19(1):157. doi:10.1186/s12974-022-02502-1
51. Ouyang L, Dan Y, Hua W, Shao Z, Duan D. Therapeutic effect of omega-3 fatty acids on T cell-mediated autoimmune diseases. *Microbiol Immunol.* 2020;64(8):563–569. doi:10.1111/1348-0421.12800
52. Adkins Y, Soulika AM, Mackey B, Kelley DS. Docosahexaenoic acid (22:6n-3) ameliorated the onset and severity of experimental autoimmune encephalomyelitis in mice. *Lipids.* 2019;54(1):13–23. doi:10.1002/lipd.12130
53. Unoda K, Doi Y, Nakajima H, et al. Eicosapentaenoic acid (EPA) induces peroxisome proliferator-activated receptors and ameliorates experimental autoimmune encephalomyelitis. *J Neuroimmunol.* 2013;256(1–2):7–12. doi:10.1016/j.jneuroim.2012.12.003
54. Bazinet RP, Laye S. Polyunsaturated fatty acids and their metabolites in brain function and disease. *Nat Rev Neurosci.* 2014;15(12):771–785. doi:10.1038/nrn3820
55. Zhang XY, Chen L, Yang Y, et al. Regulation of rotenone-induced microglial activation by 5-lipoxygenase and cysteinyl leukotriene receptor 1. *Brain Res.* 2014;1572:59–71. doi:10.1016/j.brainres.2014.05.026
56. Kong W, Hooper KM, Ganea D. The natural dual cyclooxygenase and 5-lipoxygenase inhibitor flavocoxid is protective in EAE through effects on Th1/Th17 differentiation and macrophage/microglia activation. *Brain Behav Immun.* 2016;53:59–71. doi:10.1016/j.bbi.2015.11.002
57. Zheng P, Tian X, Zhang W, et al. Rhein suppresses neuroinflammation via multiple signaling pathways in LPS-stimulated BV2 microglia cells. *Evid Based Complement Alternat Med.* 2020;2020(1):7210627. doi:10.1155/2020/7210627
58. Wen Q, Miao J, Lau N, et al. Rhein attenuates lipopolysaccharide-primed inflammation through NF-kappaB inhibition in RAW264.7 cells: targeting the PPAR-gamma signal pathway. *Can J Physiol Pharmacol.* 2020;98(6):357–365. doi:10.1139/cjpp-2019-0389
59. Jadaun KS, Mehan S, Sharma A, et al. Neuroprotective effect of chrysophanol as a PI3K/AKT/mTOR signaling inhibitor in an experimental model of autologous blood-induced intracerebral hemorrhage. *Curr Med Sci.* 2022;42(2):249–266. doi:10.1007/s11596-022-2496-x
60. Hu G, Zhou X. Gallic acid ameliorates atopic dermatitis-like skin inflammation through immune regulation in a mouse model. *Clin Cosmet Investig Dermatol.* 2021;14:1675–1683. doi:10.2147/CCID.S327825
61. Navarrete-Yanez V, Garate-Carrillo A, Rodriguez A, et al. Effects of (-)-epicatechin on neuroinflammation and hyperphosphorylation of tau in the hippocampus of aged mice. *Food Funct.* 2020;11(12):10351–10361. doi:10.1039/D0FO02438D

Drug Design, Development and Therapy

Publish your work in this journal

Drug Design, Development and Therapy is an international, peer-reviewed open-access journal that spans the spectrum of drug design and development through to clinical applications. Clinical outcomes, patient safety, and programs for the development and effective, safe, and sustained use of medicines are a feature of the journal, which has also been accepted for indexing on PubMed Central. The manuscript management system is completely online and includes a very quick and fair peer-review system, which is all easy to use. Visit <http://www.dovepress.com/testimonials.php> to read real quotes from published authors.

Submit your manuscript here: <https://www.dovepress.com/drug-design-development-and-therapy-journal>

Dovepress
Taylor & Francis Group